# A Full State Feedback Controller for Dynamic Capacitive Wireless Power Transfer Systems

**Abstract** – This digest presents a novel full-state feedback (FSF) controller for compensating changing coupling variations in dynamic capacitive wireless power transfer (WPT) systems utilizing an active variable reactance (AVR) rectifier. The AVR rectifier enables continuous compensation, allowing the WPT system to maintain high-efficiency power transfer at a fixed frequency by appropriately distributing power between its two branches. Conventional PID control is suboptimal for the AVR rectifier due to the higher-order system dynamics, nonlinearities, and cross-coupling between control loops. In contrast, the FSF control strategy presents an optimal and robust way to control higher order multi-input multi-output systems like the AVR rectifier. A state-space model is developed for the AVR rectifier, and the FSF controller is designed based on this model. To validate the proposed approach, a 13.56 MHz 100-W capacitive WPT system with an AVR rectifier is built and tested. The controller's effectiveness is demonstrated through both simulations and experiments on the hardware prototype.

## I. Introduction

Wireless power transfer is becoming increasingly important and has the potential to accelerate the widespread adoption of electric vehicles (EVs), especially amongst vehicles that routinely travel along fixed routes such as buses and warehouse forklifts. Capacitive WPT systems can be lighter, cheaper, and smaller than comparable inductive WPT systems due to the absence of ferrite cores. The ability of capacitive WPT systems to transfer high power at high efficiency has been demonstrated [1], thus proving the viability of this technology.

One main challenge of WPT systems is the extreme sensitivity to the value of the coupling capacitance or mutual inductance between the receiver and the transmitter. To increase the practicality of WPT systems in dynamic applications, it is desirable to design and control them to tolerate coupling variations while maintaining full power transfer at high efficiency. The recently proposed active variable reactance (AVR) rectifier [2] addresses these challenges and efficiently provides variable compensation in high-frequency WPT systems. However, a robust controller is needed in order to perform this compensation automatically and with a sufficiently high bandwidth to allow for in-motion dynamic EV charging. A conventional PID control-based decoupled-dual-loop strategy has been proposed in [3], [4] to compensate for changing coupling capacitance while maintaining the desired power transfer. However, such approaches are not well-suited to optimally control the AVR rectifier due to the higher-order system dynamics, nonlinearities, and cross-coupling between the two control loops.

This work presents a novel time-domain solution for the control of the AVR rectifier with sufficiently high bandwidth and robustness to operate the system dynamically. First, a model of the AVR rectifier is derived in state space. Then, a state-space control strategy is proposed, and an optimal FSF linear quadratic regulator (LQR) controller is designed and validated in simulation. Finally, a prototype 13.56-MHz, 100-W capacitive WPT system with an AVR rectifier and a dynamically variable coupling capacitance is built and its operation demonstrated with the proposed control strategy.

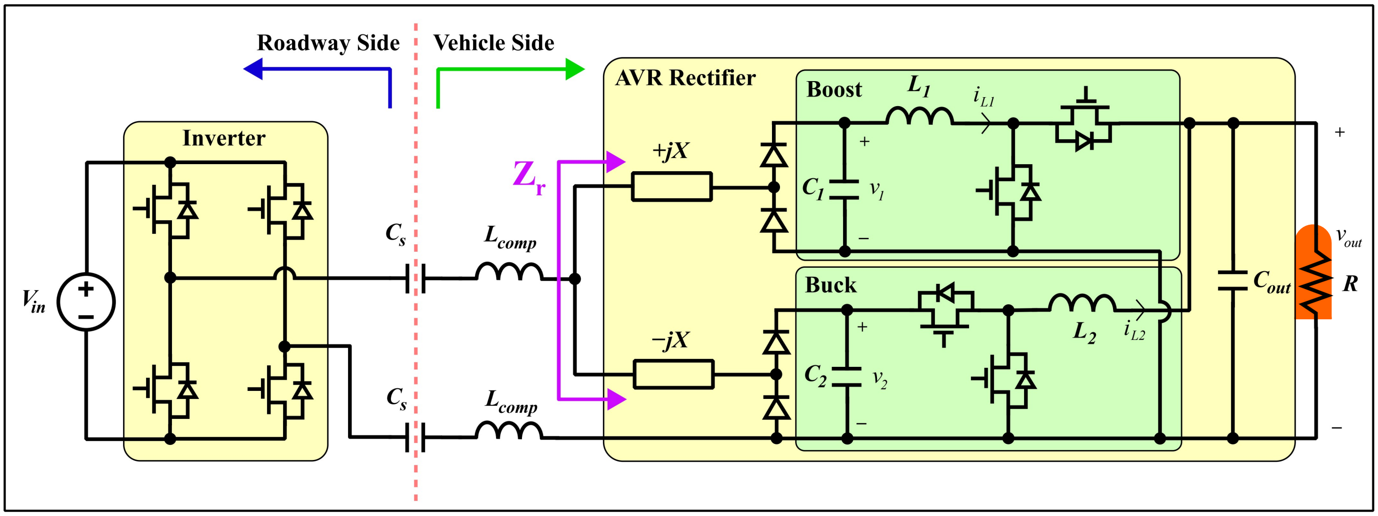


Fig. 1: Dynamic capacitive wireless power transfer system with active variable reactance rectifier schematic.

## II. Dynamic Capacitive Wireless Power Transfer System with an AVR Rectifier

Figure 1 presents the full circuit schematic of the capacitive WPT system equipped with an AVR rectifier. A DC input bus is connected to a full-bridge inverter. Power then flows through the $C_s$-$L_{comp}$ tank. $C_s$ is the coupling capacitance between the roadway-side and vehicle-side coupling plates; $L_{comp}$ is designed so that the impedance of the LC tank is zero when $C_s$ assumes its nominal value.

The AVR rectifier that follows has two parts: a top branch consisting of a boost converter pulling power through an inductive reactance $+jX$, and a bottom branch consisting of a buck converter pulling power through a capacitive reactance $-jX$. By varying the amount of power processed in each of the two branches, the AVR rectifier can control its output power $P_{out}$ and input impedance $Z_r$. It can be shown that these two quantities can be written as:

$$P_{out} = P_1 + P_2 = v_1 i_{L1} + v_{out} i_{L2} \qquad (1)$$

$$Z_r = R_r + jX_r = \frac{k_{rec}^2 v_1^2 v_2^2 + v_1 v_{out} i_{L1} i_{L2} X^2}{k_{rec}(v_1 v_2^2 i_{L1} + v_{out} v_1^2 i_{L2})} + jX \frac{v_1 i_{L1} v_2^2 - v_{out} i_{L2} v_1^2}{v_1 i_{L1} v_2^2 + v_{out} i_{L2} v_1^2} \qquad (2)$$

where $k_{rec}$ is a gain associated with the half-bridge rectifiers and $X$ is the differential reactance $\pm jX$ attached to the two branches. When the coupling capacitance $C_s$ changes by an amount $\Delta C_s$, we use Eqn. 2 to adjust the operation of the AVR rectifier such that $\mathrm{Im}(Z_r)$ perfectly compensates $\Delta C_s$ while holding $P_{out}$ constant. It can be shown that this is equivalent to holding $\mathrm{Re}(Z_r)$ constant at its nominal value when $\Delta C_s = 0$. This allows the controller to avoid estimating $\Delta C_s$ and adjusting the control target to track this value in real time.

A frequency-based controller has been proposed in [4] which utilizes two control loops: one holds $P_{out}$ constant, and the other holds $\mathrm{Re}(Z_r)$ constant. The two loops run at the same frequency, but use constant decoupling gains to minimize the impact one control action has on the other. However, the controller does not have sufficient performance to operate the system in dynamic charging scenarios; thus, a more robust controller is needed.

## III. State Space Modeling of the AVR Rectifier

In this section, a model for the AVR rectifier is developed in state space; Sec. IV uses this model for the design of a robust FSF controller. A similar modeling method is presented in [5]. Fig. 2 contains the small-signal linearized model of the AVR rectifier. Of note is the inclusion of the input capacitance on both of the converters; these capacitors are necessary in modeling the dynamics of the converter as the input voltages $v_1$ and $v_2$ vary.

In general, a continuous-time state-space model can be written as $\frac{d}{dt}\vec{x} = A\vec{x} + B\vec{u}$, where $\vec{x}$ contains the system states, $\vec{u}$ contains the system inputs, $A$ is the system dynamics matrix, and $B$ is the input dynamics matrix. First, the elements of our state vector $\vec{x}$ are chosen as the capacitor voltages and inductor currents: $v_1, v_2, i_{L1}, i_{L2}$, and $v_{out}$. The input vector $\vec{u}$ is chosen to contain $d_1$ and $d_2$, which correspond to the control handles (the duty cycles of the boost and the buck converters, respectively).

First-order differential equations for $\frac{d}{dt}\vec{x}$ are written using time-domain circuit analysis techniques. These are arranged into a matrix, resulting in a valid five-state un-augmented state space model of the AVR rectifier. However, the controller design requires additional augmented integral states $z_1 = \int_0^t (p_{out}(\tau) - P_{out})d\tau$ and $z_2 = \int_0^t (\mathrm{Re}(z_r(\tau)) - \mathrm{Re}(Z_r))d\tau$ which track the integral of the error in output power $p_{out}(t)$ and error in input impedance $\mathrm{Re}(z_r(t))$, respectively. Thus, the state vector becomes $\overrightarrow{x_{aug}} = [\vec{x}; z_1; z_2]$, and the complete state-space model becomes Eqn. 3, which is then used to design the FSF controller. This model is the first significant contribution of this digest, and a derivation will be presented in the full paper.

$$\frac{d}{dt}\begin{bmatrix} v_{out} \\ v_1 \\ v_2 \\ i_{L1} \\ i_{L2} \\ z_1 \\ z_2 \end{bmatrix} = \begin{bmatrix} -\frac{1}{RC_{out}} & 0 & 0 & \frac{D_1'}{C_{out}} & \frac{1}{C_{out}} & 0 & 0 \\ 0 & 0 & 0 & -\frac{1}{C_1} & 0 & 0 & 0 \\ 0 & 0 & 0 & 0 & -\frac{D_2}{C_2} & 0 & 0 \\ -\frac{D_1'}{L_1} & \frac{1}{L_1} & 0 & 0 & 0 & 0 & 0 \\ -\frac{1}{L_2} & 0 & \frac{D_2}{L_2} & 0 & 0 & 0 & 0 \\ -I_{L2} & -I_{L1} & 0 & -V_1 & -V_{out} & 0 & 0 \\ -\frac{\partial Re(z_r)}{\partial v_{out}} & -\frac{\partial Re(z_r)}{\partial v_1} & -\frac{\partial Re(z_r)}{\partial v_2} & -\frac{\partial Re(z_r)}{\partial i_{L1}} & -\frac{\partial Re(z_r)}{\partial i_{L2}} & 0 & 0 \end{bmatrix} \begin{bmatrix} v_{out} \\ v_1 \\ v_2 \\ i_{L1} \\ i_{L2} \\ z_1 \\ z_2 \end{bmatrix} + \begin{bmatrix} -\frac{I_{L1}}{C_{out}} & 0 \\ 0 & 0 \\ 0 & -\frac{I_{L2}}{C_2} \\ \frac{V_{out}}{L_1} & 0 \\ 0 & \frac{V_2}{L_2} \\ 0 & 0 \\ 0 & 0 \end{bmatrix} \begin{bmatrix} d_1 \\ d_2 \end{bmatrix} \quad (3)$$

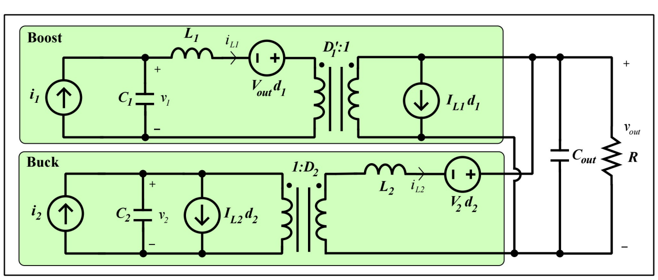


Fig. 2: Schematic of the AVR rectifier's linearized small-signal model.

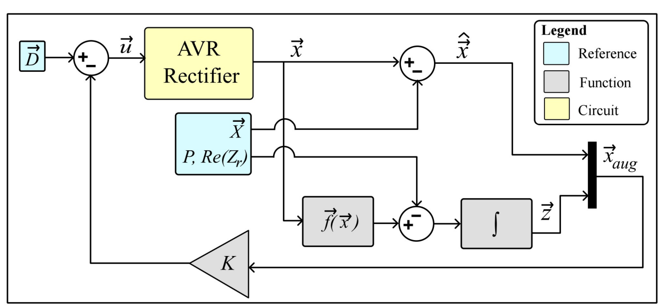


Fig. 3: Simplified block diagram of the state-space control loop. $\vec{f}(\vec{x})$ is a nonlinear function which computes $p_{out}$ and $\mathrm{Re}(z_r)$ from $\vec{x}$. Capital letters denote dc values of the parameter at the nominal coupling capacitance.

## IV. Full State Feedback Controller Design and Simulation Validation

Figure 3 shows the complete block diagram of the system under closed-loop control. The controller design consists of finding a gains matrix $K$ such that setting the input as $\vec{u} = r - K\overrightarrow{x_{aug}}$ results in the closed-loop system holding $P_{out}$ and $\mathrm{Re}(Z_r)$ constant regardless of the value of $C_s$. To find an optimal $K$, heuristic techniques presented in [6] are used to design a linear quadratic regulator (LQR) with reasonable values for the diagonal elements of the $Q$ and $R$ cost-defining matrices. Then, the `lqr()` function in MATLAB is utilized to solve the corresponding Algebraic Riccati Equation for the optimal gains matrix $K$. The design of this controller is the second significant contribution of this digest; the strategy for choosing $Q$ and $R$ will be presented in the full paper.

A model is built in Simulink and PLECS to validate the proposed controller. Fig. 4 shows the control objectives $P_{out}$ and $\mathrm{Re}(Z_r)$ being controlled to their target values of 200 W and 50 Ω, respectively, while the coupling reactance is disturbed by an amount $\Delta X_s$. The impedance seen by the inverter must be near-resistive for the converter to operate at peak efficiency. Fig. 5 shows the input voltage and current waveforms at the inverter output under a misalignment condition with and without the controller. The proposed controller is driving the input impedance effectively, as the voltage and current waveforms seen by the inverter are nearly in-phase.

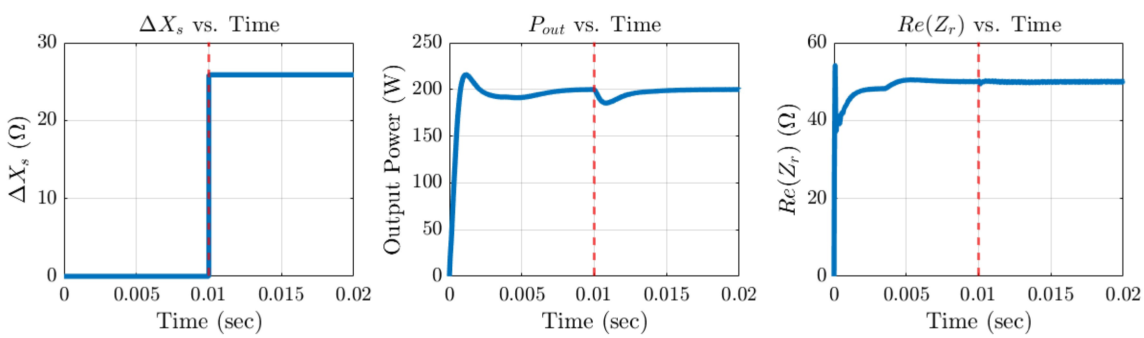


Fig. 4: $P_{out}$ and $\mathrm{Re}(Z_r)$, showing response to a step change in coupling reactance $\Delta X_s \equiv \frac{1}{2\pi f_s C_{s,nom}} - \frac{1}{2\pi f_s C_s}$, where $C_{s,nom}$ is the nominal coupling capacitance, and $f_s$ is the switching frequency in Hz.

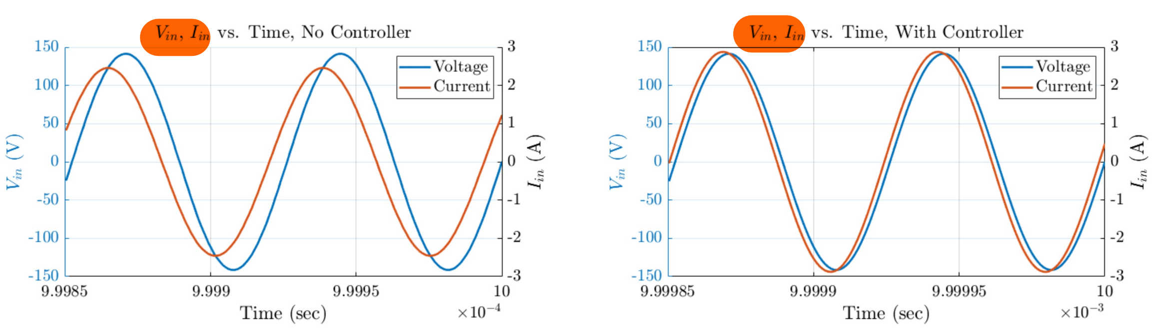


Fig. 5: $V_{in}$ and $I_{in}$ as functions of time, with a change in coupling reactance $\Delta X_s = 26\Omega$ in both cases.

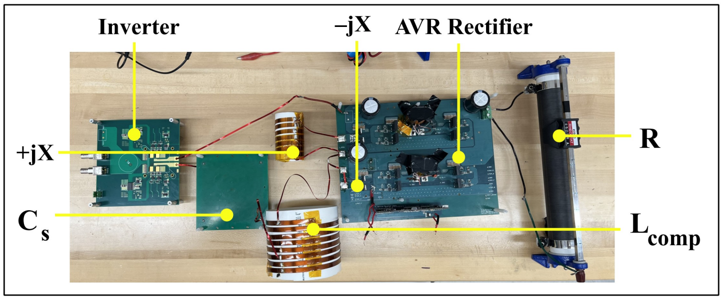


Fig. 6: Annotated photograph of the hardware prototype.

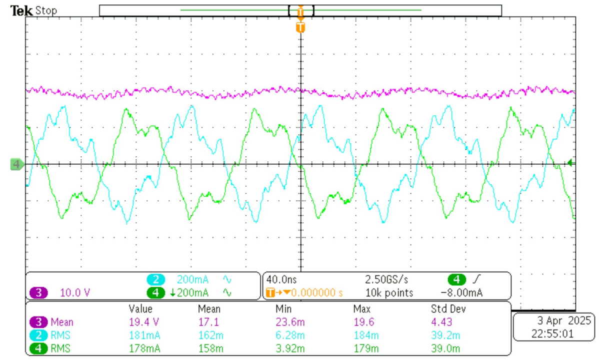


Fig. 7: Experimental waveforms showing AVR rectifier branch currents and output voltage.

## V. Hardware and Experimental Results

The proposed controller is implemented on a prototype 13.56 MHz, 100-W capacitive WPT system equipped with an AVR rectifier and a dynamically adjustable coupling capacitance. Fig. 6 shows the hardware prototype and experimental setup with annotations labeling important components. Fig. 7 shows AVR rectifier waveforms with $\Delta C_s = 0$ and $V_{in} = 30\ V$. The current flowing into the AVR rectifier is being split evenly between the $+jX$ and $-jX$ branches, showing nominal operation. The controller implementation and experimental results showing controller effectiveness comprise the third significant contribution of this digest.

## VI. Conclusion and Future Work

This digest presents a novel state-space model and full state feedback (FSF) controller for capacitive WPT systems equipped with AVR rectifiers. The proposed controller allows the system to transfer power efficiently as the coupling capacitance between the transmitter and receiver is varied. A 6.78-MHz, 100-W capacitive WPT system with an AVR rectifier and a dynamically adjustable coupling capacitance was assembled. The proposed controller was validated in simulation and on the hardware prototype.

## References

[1] S. Maji, D. Etta, and K. K. Afridi, "A high-power large air-gap multi-mhz dc-dc capacitive wireless power transfer system for electric vehicle charging," in *2023 IEEE Wireless Power Technology Conference and Expo (WPTCE)*, pp. 1–6, 2023.

[2] S. Sinha, A. Kumar, B. Regensburger, and K. K. Afridi, "Active variable reactance rectifier—a new approach to compensating for coupling variations in wireless power transfer systems," *IEEE Journal of Emerging and Selected Topics in Power Electronics*, vol. 8, no. 3, pp. 2022–2040, 2020.

[3] S. Sinha and K. K. Afridi, "Closed-loop control of a dynamic capacitive wireless power transfer system," in *2019 20th Workshop on Control and Modeling for Power Electronics (COMPEL)*, pp. 1–6, 2019.

[4] S. Maji, Y. Cao, D. Etta, and K. K. Afridi, "An intelligent control methodology for in-motion dynamic capacitive wireless power transfer systems," in *2024 IEEE Workshop on Control and Modeling for Power Electronics (COMPEL)*, pp. 1–7, 2024.

[5] J. C. Mayo-Maldonado, J. C. Rosas-Caro, R. Salas-Cabrera, A. González-Rodriguez, O. F. Ruíz-Martínez, R. Castillo-Gutiérrez, J. R. Castillo-Ibarra, and H. Cisneros-Villegas, "State space modeling and control of the dc-dc multilevel boost converter," in *2010 20th International Conference on Electronics Communications and Computers (CONIELECOMP)*, pp. 232–236, 2010.

[6] R. Williams and D. Lawrence, *Linear State-Space Control Systems*. Wiley, 2007.